Urban heat island impacts on heat-related cardiovascular morbidity: A time series analysis of older adults in US metropolitan areas

Stephanie E. Cleland[a,b], **William Steinhardt**[b], **Lucas M. Neas**[c], **J. Jason West**[a], **Ana G. Rappold**[c,*]

[a]Department of Environmental Sciences and Engineering, Gillings School of Global Public Health, University of North Carolina, Chapel Hill, NC, USA

[b]Oak Ridge Institute for Science and Education at the Center for Public Health and Environmental Assessment, Office of Research and Development, United States Environmental Protection Agency, Research Triangle Park, NC, USA

[c]Center for Public Health and Environmental Assessment, Office of Research and Development, United States Environmental Protection Agency, Research Triangle Park, NC, USA

Abstract

Many United States (US) cities are experiencing urban heat islands (UHIs) and climate change-driven temperature increases. Extreme heat increases cardiovascular disease (CVD) risk, yet little is known about how this association varies with UHI intensity (UHII) within and between cities. We aimed to identify the urban populations most at-risk of and burdened by heat-related CVD morbidity in UHI-affected areas compared to unaffected areas. ZIP code-level daily counts of CVD hospitalizations among Medicare enrollees, aged 65–114, were obtained for 120 US metropolitan statistical areas (MSAs) between 2000 and 2017. Mean ambient temperature exposure was estimated by interpolating daily weather station observations. ZIP codes were classified as low and high UHII using the first and fourth quartiles of an existing surface UHII metric, weighted to each have 25% of all CVD hospitalizations. MSA-specific associations

*Corresponding author at: U.S. EPA Human Studies Facility, 104 Mason Farm Rd., Chapel Hill, NC 27514, USA. rappold.ana@epa.gov (A.G. Rappold).

Disclaimer

Although this work has been reviewed for publication by the U.S. Environmental Protection Agency, it does not necessarily reflect the views and policies of the Agency.

Declaration of Competing Interest

The authors declare that they have no known competing financial interests or personal relationships that could have appeared to influence the work reported in this paper.

CRediT authorship contribution statement
Stephanie E. Cleland: Conceptualization, Methodology, Data curation, Formal analysis, Investigation, Software, Validation, Visualization, Writing – original draft, Writing – review & editing. **William Steinhardt:** Data curation, Software, Writing – review & editing. **Lucas M. Neas:** Conceptualization, Methodology, Investigation, Writing – review & editing. **J. Jason West:** Conceptualization, Writing – review & editing. **Ana G. Rappold:** Conceptualization, Methodology, Investigation, Supervision, Project administration, Writing – review & editing.

between ambient temperature and CVD hospitalization were estimated using quasi-Poisson regression with distributed lag non-linear models and pooled via multivariate meta-analyses. Across the US, extreme heat (MSA-specific 99th percentile, on average 28.6 °C) increased the risk of CVD hospitalization by 1.5% (95% CI: 0.4%, 2.6%), with considerable variation among MSAs. Extreme heat-related CVD hospitalization risk in high UHII areas (2.4% [95% CI: 0.4%, 4.3%]) exceeded that in low UHII areas (1.0% [95% CI: −0.8%, 2.8%]), with upwards of a 10% difference in some MSAs. During the 18-year study period, there were an estimated 37,028 (95% CI: 35,741, 37,988) heat-attributable CVD admissions. High UHII areas accounted for 35% of the total heat-related CVD burden, while low UHII areas accounted for 4%. High UHII disproportionately impacted already heat-vulnerable populations; females, individuals aged 75–114, and those with chronic conditions living in high UHII areas experienced the largest heat-related CVD impacts. Overall, extreme heat increased cardiovascular morbidity risk and burden in older urban populations, with UHIs exacerbating these impacts among those with existing vulnerabilities.

Keywords

Urban heat island; Extreme heat; Cardiovascular disease; Hospitalization; United States; Medicare

1. Introduction

Approximately 30% of the world's population are exposed to deadly heat each year (Mora et al., 2017). Exposure to extreme heat events among urban populations has nearly tripled since the 1980s, impacting around 1.7 billion people (Tuholske et al., 2021). Urban areas are home to the majority of the population worldwide (United Nations Department of Economic and Social Affairs, 2018) and with climate change, increased urbanization, and population ageing, cities are expected to bear the brunt of rising temperatures (Tong et al., 2021). This is in part due to the higher temperatures experienced in heavily urbanized areas, known as urban heat islands (UHIs), a phenomenon largely caused by an increased presence of heat-retaining buildings and pavement and decreased greenspace (Mohajerani et al., 2017; Oke et al., 2017; Rizwan et al., 2008).

Exposure to high temperatures and heat waves are associated with increased all-cause and cause-specific morbidity and mortality (Green et al., 2019; Song et al., 2017). Specifically, a large body of epidemiologic evidence shows that short-term heat exposure elevates the risk of mortality from cardiovascular disease (CVD) (Song et al., 2017), especially among older adults (Åström et al., 2011; Bunker et al., 2016; Son et al., 2019). The biological mechanisms by which heat reduces cardiovascular function are well understood, with high temperatures altering blood pressure, heart rate, and blood viscosity (Gostimirovic et al., 2020). However, there is inconsistent evidence of the impact of heat exposure on cardiovascular morbidity (Cicci et al., 2022; Phung et al., 2016; Turner et al., 2012; Weilnhammer et al., 2021). Additionally, few epidemiologic studies have investigated the modification of heat-related cardiovascular morbidity risk by individual factors beyond age and sex, such as comorbidities (Bai et al., 2018, 2016; Lam et al., 2018) or race, both of which can impact heat vulnerability (Gronlund, 2014). In the US, urban areas are racially

diverse (Cromartie, 2018) and home to many people with chronic conditions (Boersma et al., 2020), emphasizing the importance of understanding the effects of heat in these populations. Previous studies also provide limited evidence of the variation in this risk within and across different urban areas in the US. It remains unclear which cities and urban populations experience the highest cardiovascular morbidity impacts during extreme heat events.

The UHI phenomenon can exacerbate the adverse health effects of extreme heat (Goggins et al., 2012; Heaviside et al., 2017; Zhao et al., 2018a; Zhu et al., 2021). UHI-related increases in temperatures are estimated to have caused 30% or more of heat-related deaths in cities in Vietnam, England, and China (Dang et al., 2018; Heaviside et al., 2016; Huang et al., 2020). This exacerbation is largely driven by UHIs increasing peak daytime temperatures and reducing overnight cooling, exposing populations in the urban core, who are often more vulnerable and socially disadvantaged (Hsu et al., 2021; Macintyre et al., 2018), to dangerously high temperatures (Heaviside et al., 2017). With urban expansion and global warming, UHIs will likely affect an increasing proportion of the urban population (Huang et al., 2019). However, the few studies that have explicitly investigated the health impacts of UHIs focused solely on mortality and produced mixed results (Dang et al., 2018; Goggins et al., 2012; Ho et al., 2023; Hondula et al., 2012; Milojevic et al., 2016; Taylor et al., 2015). In the face of increasing ambient temperatures and intensifying UHIs, a clearer understanding of whether UHIs exacerbate heat-related cardiovascular morbidity, and identifying populations within UHI-affected areas that are the most vulnerable to and burdened by high temperatures, is essential.

We evaluated the heat-related risk and burden of cardiovascular morbidity among older urban populations and explored how the observed impacts varied with surface UHI intensity (UHII) within and between cities. Specifically, a time series approach was used to estimate the impact of extreme heat on CVD hospitalizations among the Medicare population living in areas affected by UHIs, compared to those living in unaffected areas, in 120 metropolitan areas within the contiguous US. We estimated both US-wide and metropolitan area-specific risks and burden and evaluated these impacts by vulnerabilities of the urban population. This is one of the first multi-city studies to investigate the cardiovascular morbidity risk and burden associated with elevated temperatures in UHIs and explore if the combined impacts of heat and UHIs vary geographically and demographically. By identifying the most heat-vulnerable urban populations and clarifying the role of UHIs, our findings may be useful for identifying areas for intervention and informing localized, targeted, and context-specific mitigation and adaptation strategies.

2. Methods

2.1. Study area

To examine the heat-cardiovascular morbidity associations in urban populations, we identified 120 metropolitan statistical areas (MSAs; defined by the US Office of Management and Budget [OMB]) in the contiguous US with a total 2010 population of 500,000 or more (Fig. 1, Table S1). Following OMB definitions, MSAs that contained an urban area with a population greater than 2.5 million were subdivided into metropolitan divisions, which function as distinct areas with substantial populations, and considered as

separate MSAs. The analysis was restricted to ZIP codes that overlapped an urbanized area (an area with a total population of 50,000 or more, as defined by the US Census Bureau) within one of the 120 MSAs, hereafter referred to as an urban core.

2.2. Study population and cardiovascular outcome

We conducted a retrospective analysis of CVD hospitalizations among Medicare enrollees, aged 65 to 114, in the 120 MSAs between 2000 and 2017. ZIP code-level daily counts of CVD-related hospitalizations were obtained using Medicare billing claims from short-stay, inpatient hospitalizations. CVD-related hospitalizations were identified using the International Classification of Diseases (ICD), Ninth Revision (ICD-9) and ICD, Tenth Revision (ICD-10) diagnosis codes (ICD-9: 390–438, ICD-10: I00-I69), which needed to be listed in one of the first three diagnosis codes on the billing claim. Hospitalizations were excluded if they occurred within four days of a previous hospitalization for CVD, as these hospitalizations were unlikely to be independent events.

To identify vulnerable population groups, we constructed subpopulation counts of CVD hospitalizations by age (65–74, 75–84, 85–114), sex (male, female), race (white, black), diabetes status (yes, no), and chronic kidney disease (CKD) status (yes, no). Diabetes and CKD were selected as comorbidities of interest because they are prevalent chronic conditions known to be heat-associated (Johnson et al., 2019; Vallianou et al., 2021). Hospitalization counts by chronic condition status were constructed to include all individuals diagnosed with the condition of interest prior to or during the study period. As such, these counts included enrollees at all stages of the chronic disease, capturing susceptibility prior to official diagnosis.

Finally, the size of the population at-risk was captured by using annual ZIP code-level counts of the number of Medicare beneficiaries, overall and for each subpopulation. The ZIP-code level daily counts of CVD hospitalizations and annual counts of beneficiaries were calculated using information on the current and end-of-year residence of an individual, respectively. The subpopulation hospitalization and beneficiary counts did not sum to the total counts due to groups not considered in the analyses (for example, those with race other than black or white) and the exclusion of a limited number of ZIP codes with an annual subpopulation beneficiary count of zero during the study period. For most subpopulations, less than 1% of ZIP codes were excluded due to insufficient beneficiary counts.

2.3. Ambient temperature data

We interpolated weather station observations of daily mean ambient temperature and relative humidity (RH), downloaded from the National Oceanic and Atmospheric Administration's National Climatic Data Center's Global Surface Summary of the Day database (National Oceanic and Atmospheric Administration, 2022), to census tract population centroids using thin-plate spline regressions for each day between 2000 and 2017. Daily mean ambient temperature, calculated using hourly observations, was selected as the exposure of interest because the 24-hour mean is often a better predictor of heat wave-related morbidity (Xu et al., 2018) and frequently used in epidemiologic analyses of non-optimal temperatures (Bunker et al., 2016). A 10-fold cross-validation of the interpolated data resulted in very

high R^2 values for temperature and relatively high R^2 values for RH. The census tract-level estimates were aggregated to the ZIP code level using population weighting:

$$Temp_{ZIP_{i,t}} = \sum_{c \in ZIP_i} Temp_{c,t} * \frac{Pop_c}{Pop_{ZIP_i}} \tag{1}$$

where $Temp_{ZIP_{i,t}}$ is the population-weighted ambient temperature in ZIP code i on day t. $Temp_{c,t}$ is the mean ambient temperature on day t in census tract c with a population centroid located within ZIP code i, and Pop_c and Pop_{ZIP_i} are the total census tract and ZIP code population, respectively, obtained using census tract-level estimates from the 2010 US Census. Population weighting gives proportionally greater weight to the temperatures experienced in more densely populated areas. ZIP code-level estimates of daily mean RH, used as a covariate in the epidemiologic model, were produced using the same approach described above. In total, temperature and RH measurements from 3,208 weather stations across the contiguous US were used (Fig. S1), with approximately 1,100–1,750 stations providing data for a given day.

2.4. Surface urban heat island intensity data

We used an existing measure of surface UHII to identify UHI and non-UHI ZIP codes. Specifically, we used estimates of census tract-level surface UHII in US urbanized areas averaged over 2013–2017 (Chakraborty et al., 2020). This UHII metric was calculated as the difference in daytime land surface temperature (LST; measured in °C) during June-August between urban and non-urban areas within each urbanized area (Chakraborty et al., 2020; Chakraborty and Lee, 2019). The June-August daytime estimates were selected to represent UHII during the hot weather season in the US and have been previously used to characterize UHIs (Hsu et al., 2021; Johnson, 2022; Romitti et al., 2022). Chakraborty et al. calculated the UHII metric using LSTs from the Moderate Resolution Imaging Spectroradiometer (MODIS) on the Aqua satellite at an 8-day temporal resolution and 1,000-meter spatial resolution. Land cover data at a 300-meter spatial resolution from the European Space Agency's Climate Change Initiative was used by Chakraborty et al. in the UHII calculation to identify the urban (built-up pixels) and non-urban (non-built-up, non-water pixels) areas in each urbanized area. We used the census tract-level estimates to generate population-weighted estimates of UHII for each ZIP code included in the analysis, using the population weighting approach (Equation (1)). To identify the areas with the lowest and highest surface UHII across the 120 MSAs, ZIP codes were classified into UHII quartiles, which were weighted to each have approximately 25% of all CVD hospitalizations to account for the higher population density in heavily urbanized areas. While this classification approach meant that not all MSAs had ZIP codes in each UHII quartile, it ensured that the first and fourth quartiles identified the most and least UHI-affected urban areas.

2.5. Epidemiologic analyses

The first aim of the epidemiologic analyses was to use year-round daily ambient temperature and hospitalization data to estimate the CVD hospitalization risk for the Medicare population associated with short-term exposure to high temperatures in US urban cores.

This association was estimated in each MSA and across all 120 MSAs using a two-stage time series modeling approach, described below. This approach was applied to the entire study population and each subpopulation separately (by age, sex, race, diabetes status, and CKD status). The second aim was to evaluate heat-related risk in the areas with the highest and lowest UHII, defined using weighted quartiles (Burkart et al., 2016; Gronlund et al., 2016; Heo et al., 2021). The two-stage modeling approach was applied to ZIP codes in the first and fourth quartiles of surface UHII (hereafter referred to as low and high UHII, respectively) to obtain UHII-specific associations in each MSA and across all MSAs. This low and high UHII analysis was conducted on the overall and subpopulation counts.

The first stage of the modeling approach applied a time-series quasi-Poisson regression with a distributed lag non-linear model (DLNM), which can concurrently represent both a non-linear exposure–response association and a non-linear lag-response association (Gasparrini, 2014). The DLNM was used to estimate the relative risk (RR) of hospitalization in response to heat exposure within each MSA. The DLNM evaluated the cumulative effect over 21-days to investigate the hypothesis that CVD hospitalizations may occur in the days and weeks following exposure and identify which days pose the greatest risk. A 21-day interval has been used in prior analyses examining the impact of year-round ambient temperature on cardiovascular outcomes (Iñiguez et al., 2021; Martinez-Solanas and Basagana, 2019; Wang et al., 2021). The DLNM can be described as follows:

$$
\begin{aligned}
\mathrm{Log}(\mathrm{E}(Y_{i,t})) =\ & \infty + cb(Temp_{i,t}, n(lag) = 21) \times \beta + ns(RH_{i,t}, df = 3) \\
& + ns(Time, df = 7/year) + DOW_t + Holiday_t + UHII_i \\
& + offset(\log(NumBeneficiaries_{i,y}))
\end{aligned}
\tag{2}
$$

where $\mathrm{E}(Y_{i,t})$ is the expected count of CVD hospitalizations on day t in ZIP code i within a given MSA, $\propto$ is the intercept, $cb(Temp_{i,t}, n(lag) = 21)$ is the cross-basis matrix of population-weighted ambient temperature in ZIP code i on day t with 21 lag days, and β is the vector of coefficients for the cross-basis. The exposure–response association in the cross-basis was defined using a natural cubic spline with three internal knots placed at the 10th, 75th, and 90th percentiles of the MSA-specific temperature distributions (Iñiguez et al., 2021; Scovronick et al., 2018; Yang et al., 2015). The lag-response association in the cross-basis was defined using a natural cubic spline with three internal knots spaced equally on the log scale (Iñiguez et al., 2021; Martinez-Solanas and Basagana, 2019; Wang et al., 2021). The DLNM also controlled for: RH, where $ns(RH_{i,t}, df = 3)$ is a natural cubic spline of population-weighted RH in ZIP code i on day t with three degrees of freedom (df) (Cui et al., 2019; Guo et al., 2017; Lu et al., 2020); seasonal and long-term trends, where $ns(Time, df = 7/year)$ is a natural cubic spline of time with seven df per year (Bai et al., 2018; Cui et al., 2019; Wang et al., 2021); day of the week, where DOW_t is a categorical variable for day t (1, 2, … 7), with 1 (Monday) as the reference (Guo et al., 2017; Martinez-Solanas and Basagana, 2019; Wang et al., 2021); holidays, where $Holiday_t$ is a categorical variable indicating whether day t is a US Federal holiday or not (1 or 0) (Cui et al., 2019; Guo et al., 2017; Martinez-Solanas and Basagana, 2019); and UHII, where $UHII_i$ is a categorical variable indicating the UHII quartile for ZIP code i, with the first quartile (low UHII) as the reference. Finally, $offset(\log(NumBeneficiaries_{i,y}))$ is an offset

for the number of beneficiaries in ZIP code *i* in year *y*, adjusting for spatial and temporal differences in Medicare population size.

The second stage used a multivariate meta-analysis to generate a pooled estimate of RR across all MSAs, using the MSA-specific average ambient temperature and temperature range as predictors (Gasparrini et al., 2015; Scovronick et al., 2018). The pooled association was used to identify the ambient temperature percentile with the lowest risk of CVD hospitalization, the minimum hospitalization percentile (MHP), which may be considered an optimum temperature percentile. A 95% confidence interval (CI) for the MHP was calculated using an approximate parametric bootstrap estimator (Tobías et al., 2017). Once the MHP was identified, the pooled association was re-centered at this value. The meta-analytical model was also used to derive a best linear unbiased prediction of the RR for each MSA. The best linear unbiased prediction allows MSAs with less data to borrow information from MSAs with more hospitalizations and similar average temperatures and temperature ranges, providing more informed estimates of the MSA-specific associations (Gasparrini et al., 2015, 2012). These updated MSA-specific associations were centered at the MHP identified in the pooled association (Iñiguez et al., 2021; Lu et al., 2020; Martinez-Solanas and Basagana, 2019), meaning each MSA had the same MHP, but a different minimum hospitalization temperature (MHT) given each MSA's unique ambient temperature distribution.

The primary results reported are: the cumulative exposure–response associations across 21 days (lags 0–20); the RR of hospitalization at the 99th ambient temperature percentile compared to the MHP, obtained from the cumulative associations; and the lag-response associations at the 99th ambient temperature percentile. The 99th percentile of MSA-specific ambient temperature distributions (hereafter referred to as extreme heat) was used as a proxy for extreme heat exposure (Hurtado-Díaz et al., 2019; Martinez-Solanas and Basagana, 2019; Wang et al., 2021). We reported both the pooled and the MSA-specific results overall and for low and high UHII areas and solely the pooled results for the subpopulation analyses. While we did not test for significant differences in RRs between groups, we did report qualitative comparisons.

Multiple sensitivity analyses were run to assess the robustness of the results to the modeling choices, including the maximum number of lag days (7, 10, 14, or 28 instead of 21), the knot placement for the exposure–response association (10th–50th–90th, 25th–50th–75th, or 10th–25th–75th–90th percentiles instead of 10th–75th–90th), the *df* used to control for seasonal and long-term trends (10 or 8 *df* instead of 7), and the number of knots used in the lag-response association (4 or 5 knots instead of 3). Additionally, daily maximum ambient temperature and daily mean apparent temperature, calculated using the RH data and the US National Weather Service's function (US National Weather Service, 2022), were considered as the exposure of interest instead of daily mean ambient temperature.

2.6. Health burden analyses

We estimated the number of heat-related CVD hospitalizations that occurred in US urban cores, overall, in low and high UHII areas, and within subpopulations, between 2000 and 2017. Using an attributable risk calculation that is an extension of the DLNM approach, and

relying on the backwards approach (Gasparrini and Leone, 2014; Guo et al., 2017; Liu et al., 2018), attributable burden was calculated as:

$$AN_{i,t} = \left(1 - \exp\left(-\sum_{l=0}^{L} \beta_{x_{t-l},l}\right)\right) * n_{i,t} \tag{3}$$

where $AN_{i,t}$ is the number of attributable CVD hospitalizations and $n_{i,t}$ is the total number of CVD hospitalizations in ZIP code i on day t. $\beta_{x_{t-l,l}}$, estimated in Equation (2), is the MSA-specific risk, which ZIP code i belongs to, associated with ambient temperature x_{t-l} at lag l. L is equal to 21 days, the maximum lag interval. To restrict the burden estimates to high temperatures, $x_{t-l} \in r$, where r is a range of ambient temperature. The temperature range, r, was set to the MHP and above to calculate the heat-attributable CVD burden (Bai et al., 2018; Gasparrini et al., 2015; Scovronick et al., 2018; Wang et al., 2021). Empirical 95% CIs for the burden estimates were obtained through Monte Carlo simulations, using 1,000 iterations and assuming a multivariate normal distribution of the MSA-specific coefficients (Martínez-Solanas et al., 2021; Mistry et al., 2022). The total heat-related CVD burden and associated 95% CI were calculated by summing $AN_{i,t}$ and the Monte Carlo simulations across all days and ZIP codes.

The number of heat-attributable CVD hospitalizations was estimated by applying Equation (3) to the subpopulation- and UHII-specific counts and associations. The primary results reported are: the heat-attributable number (AN), the number of CVD hospitalizations attributable to temperatures above the MHP; and the annual heat-attributable rate (AR), the average annual AN per 100,000 beneficiaries. We report the total and MSA-specific burden for the entire study population, overall and in low and high UHII areas, and solely the total burden for the subpopulations. The AN can be used to compare the absolute burden for each MSA, subpopulation, and UHII level, while the AR can be used to compare the relative burden, accounting for differences in population size. The subpopulation- and UHII-specific ANs did not sum to the overall AN because each estimate relied on their unique RRs.

Both the epidemiologic and health burden analyses were conducted in R (version 4.0.3; R Development Core Team), using the packages 'dlnm' (Gasparrini, 2011) and 'mvmeta' (Gasparrini et al., 2012) and the functions 'attrdl.R' (Gasparrini and Leone, 2014) and 'findmin.R' (Tobías et al., 2017).

3. Results

3.1. Study population & exposure data

A total of 48.6 million CVD hospitalizations over 2000–2017 were identified among approximately 21.6 million total beneficiaries in 9,917 ZIP codes (Table 1). ZIP codes classified as low UHII areas had a surface UHII between −9.3 °C and 0.5 °C. ZIP codes classified as high UHII areas had a surface UHII between 3.9 °C and 10.3 °C. On average, high UHII areas had an UHII of 5.6 °C, meaning summer daytime LSTs were approximately 5.6 °C warmer in these areas compared to their non-urban reference areas. Most ZIP codes with high UHII were centrally located in the urban cores of the MSAs, while ZIP codes

with low UHII were located near the edges (Fig. 1). Low and high UHII areas had an equal number of CVD hospitalizations, but high UHII areas had fewer enrollees located in less ZIP codes (Table 1), indicating a denser and more frequently hospitalized Medicare population in high UHII areas. The proportion of hospitalizations indicates that the Medicare population in high UHII areas is generally older, more female, more non-white, and with more chronic conditions.

Across the 120 MSAs and 18-year study period, the average daily mean ambient temperature was 14.8 °C (Interquartile range [IQR]: 14.1 °C) and the 99th percentile of daily mean ambient temperature was 28.6 °C. While low and high UHII areas had different surface UHIIs, they had the same average daily mean ambient temperature of 14.4 °C (IQR: 14.1 °C for both). The two areas also had similar 99th percentiles of daily mean ambient temperature, with 28.4 °C for low and 28.3 °C for high UHII areas. Details on the region, climate, temperature, and study population of the 120 MSAs can be found in Table S1. Additional maps of ZIP code-level hospitalization counts, temperature, and UHII can be viewed in Fig. S2–4 or online at: https://shiny.stat.ncsu.edu/Heat-CVD-UHI-Dashboard/.

3.2. Overall risk and burden

Pooled across the 120 MSAs, extreme heat (MSA-specific 99th temperature percentile, on average 28.6 °C) increased the 21-day cumulative RR of CVD hospitalization by 1.5% (95% CI: 0.4%, 2.6%) (Fig. 2A–B, Table S2). A U-shaped association was observed, with the MHP located at the 92nd percentile (95% CI: 90, 95; on average 25.7 °C [95% CI: 25.2 °C, 26.5 °C]) (Fig. 3). The lag-response association for extreme heat revealed an initial risk at lag 0, followed by a slightly delayed association, with risk peaking at lag 5 and continuing until lag 12. While many MSAs exhibited a similar U or J-shaped association (Fig. S5), there was considerable variation in the MSA-level MHTs and RRs (Fig. 4, S6, S7, Table S3), with MHTs ranging from 18.9 °C to 35.3 °C and extreme heat-related RRs ranging from a 10.4% decrease to a 16.5% increase in CVD hospitalization risk. Approximately two-thirds of MSAs had increased risk of CVD hospitalizations, with 20% having a significant increase (Fig. S8).

The estimated 37,028 (95% CI: 35,741, 37,988) CVD hospitalizations attributable to heat exposure over the 18-year study period accounted for an average of 9.52 (95% CI: 9.19, 9.76) heat-attributable CVD admissions per 100,000 beneficiaries each year (Fig. 2C–D, Table S2). The MSAs that experienced the highest total burden were those with high RRs, steep risk curves (that is, a sharper increase in risk per degree change in temperature), and a high number of total CVD hospitalizations (Figs. S5–7; Table S3). There was no apparent spatial, regional, or climactic patterns in the MSA-level heat-attributable CVD risk and burden (Figs. S9, S10). The heat-related CVD hospitalization risk and burden, overall and for each MSA, can also be viewed online at: https://shiny.stat.ncsu.edu/Heat-CVD-UHI-Dashboard/.

3.3. Overall risk and burden in subpopulations

While extreme heat increased the risk of CVD hospitalizations across most subpopulations, older (age 85–114), black, and female enrollees, those with CKD, and those with diabetes

generally had slightly lower MHPs, steeper risk curves, and higher extreme heat-related RR (Fig. 2A–B, S11–15, Table S2). For example, extreme heat increased the 21-day cumulative RR by 2.4% (95% CI: 1.3%, 3.5%) for those with CKD, compared to 0.7% (95% CI: −0.3%, 1.7%) for those without. Similarly, the extreme heat-related RRs were moderately higher for females (2.1% [95% CI: 0.8%, 3.5%]) than males (0.7% [95% CI: −0.3%, 1.7%]); for older (age 85–114) enrollees (2.8% [95% CI: 1.3%, 4.2%]) than younger (age 65–74) enrollees (0.1% [95% CI: −1.0%, 1.3%]); and for black enrollees (2.4% [95% CI: 0.7%, 4.1%]) than white enrollees (1.3% [95% CI: 0.2%, 2.5%]). The extreme heat lag-response associations also varied by subpopulation, with a slightly quicker response in the populations at higher risk (Figs. S11–15).

The heat-attributable CVD burden was also larger in more vulnerable subpopulations. For example, enrollees with CKD accounted for almost 79% (AN: 29,113 [95% CI: 28,279, 29,678]) of the total heat-related burden, leading to 6 times more heat-attributable CVD admissions per 100,000 beneficiaries each year than those without CKD (AR: 23.56 [95% CI: 22.89, 24.02] for CKD vs. 3.87 [95% CI: 3.71, 3.97] for non-CKD). Similarly, females and those with diabetes accounted for approximately 73% (AN: 27,200 [95% CI: 26,205, 27,910]) and 78% (AN: 25,249 [95% CI: 24,450, 25,801]) of the total heat-related CVD burden, respectively, with higher ARs than males and those without diabetes. The heat-attributable burden also increased with age, with enrollees aged 85–114 having the highest AR (34.76 [95% CI: 33.50, 35.61]) and accounting for approximately 41% (AN: 15,381 [95% CI: 14,822, 15,757]) of the total heat-related CVD burden. While white enrollees had a higher AN (approximately 63% of total burden; 23,438 [95% CI: 22,435, 24,167]), reflecting the larger number of white enrollees, black enrollees had a higher AR, with more than double the number of heat-attributable CVD admissions per 100,000 beneficiaries each year (AR: 17.46 [95% CI: 16.63, 18.09] for black vs. 7.51 [95% CI: 7.19, 7.74] for white). The subpopulation-specific heat-related risk and burden can also be viewed online at: https://shiny.stat.ncsu.edu/Heat-CVD-UHI-Dashboard/.

3.4. Risk and burden difference by urban heat island intensity

Pooled across all MSAs, high UHII areas, compared to low UHII areas, had a moderately lower MHP, steeper risk curve, higher extreme heat-related RR, and more immediate extreme heat lag-response association (Fig. 2A–B, Fig. 3, Table S2). Specifically, extreme heat increased the 21-day cumulative RR of CVD hospitalization by 2.4% (95% CI: 0.4%, 4.3%) in high UHII areas, compared to 1.0% (95% CI: −0.8%, 2.8%) in low UHII areas. There were substantial differences in UHII-level extreme heat-related CVD risk between MSAs, with no clear spatial, regional, or climactic trends (Figs. S10, S16). Approximately half of MSAs had at least a 1% higher, and up to a 10% higher, extreme heat-related CVD hospitalization RR in high UHII areas (Fig. 4, S7, Table S3). For high UHII areas, 78% of MSAs had an increase in CVD hospitalization RR associated with extreme heat, compared to 60% for low UHII.

There was a notably higher heat-related CVD burden in high UHII areas in comparison to low UHII areas (Fig. 2C–D), with over 11,000 more heat-attributable CVD admissions (AN: 12,834 [95% CI: 12,012, 13,452] in high vs 1,423 [95%: 480, 2,111] in low) and 11 times

more heat-related CVD admissions per 100,000 beneficiaries each year (AR: 14.86 [95% CI: 13.91, 15.58] in high vs. 1.34 [95% CI: 0.45, 1.98] in low). While high and low UHII areas each accounted for 25% of all CVD hospitalizations, high UHII areas accounted for approximately 35% of the total heat-related CVD burden while low UHII areas accounted for 4%.

Vulnerable subpopulations generally had a more pronounced extreme heat-related CVD risk in high UHII areas, compared to a minimal difference in UHII-level risk for low-risk subpopulations (Fig. 2A–B, S11–15, Table S2). The largest difference in extreme heat-related CVD risk by UHII level was observed for female enrollees, who had a 3.6% (95% CI: 1.3%, 5.8%) increase CVD hospitalization RR in high UHII areas, compared to 0.5% (95% CI: −1.2%, 2.2%) in low UHII areas. In contrast, male enrollees had a 0.9% (95% CI: −1.0%, 2.8%) increase in high UHII areas and a 1.1% (95% CI: −1.0%, 3.3%) increase in low UHII areas. Similar differences in extreme heat-related CVD hospitalization RR by UHII level was also observed among enrollees with CKD and enrollees with diabetes, compared to no discernable differences among those without. Across the age groups, enrollees aged 75–84 had the largest difference in UHII-specific risk, with an elevated extreme heat-related CVD hospitalization risk in high UHII areas (RR: 2.8% [95% CI: 0.1%, 5.5%] in high vs. −0.1% [95% CI: −0.8%, 0.7%] in low). There were no notable differences in risk between low and high UHII areas by Medicare enrollee race.

High-risk groups also had a notably elevated heat-related CVD burden in high UHII areas (Fig. 2C–D). Enrollees with diabetes in high UHII areas accounted for 40% (AN: 9,999 [95% CI: 9,432, 10,443]) of the total diabetes-specific heat-related CVD burden, with 6 times more heat-attributable CVD admissions per 100,000 beneficiaries each year than those in low UHII areas (AR: 29.56 [95% CI: 27.88, 30.87] in high vs. 4.71 [95% CI: 3.16, 5.72] in low). In comparison, those without diabetes in high UHII areas accounted for 25% (AN: 2,773 [95% CI: 2,426, 3,002]) of the non-diabetes-specific heat-related CVD burden. These marked discrepancies in UHII-specific burden also occurred in female enrollees and those with CKD. Enrollees aged 75–84 in high UHII areas had the highest AN across all age groups and UHII levels, with high UHII accounting for 53% (AN: 5,863 [95% CI: 5,357, 6,251]) of the total age 75–84-specific heat-related CVD burden. Enrollees aged 85–114 in high UHII areas had the highest AR (45.85 [95% CI: 43.82, 47.37]). While black and white enrollees had similar differences in AN and AR in high versus low UHII areas, high UHII areas accounted for approximately 56% (3,813 [95%: 3,594, 3,982]) of the total black-specific AN and only 32% (7,436 [95% CI: 6,752, 7,950]) of the total white-specific AN, reflecting the higher percentage of black enrollees in high UHII areas. Results for the heat-related CVD risk and burden by UHII level, overall and for each MSA and subpopulation, can also be viewed online at: https://shiny.stat.ncsu.edu/Heat-CVD-UHI-Dashboard/.

3.5. Sensitivity analyses

Multiple sensitivity analyses were run to evaluate the robustness of the cardiovascular risk and burden analyses (Table S4, Fig. S17). Overall, the results were generally insensitive to the model specification and parameters. When different *df* were used to control for seasonal and long-term time trends, the extreme heat-related RR, as well as the AN and

AR, remained consistent with the primary findings, except for a small decrease in the steepness of the exposure–response risk curve (Fig. S18). Similarly, when the maximum lag was changed in the model or when more knots were used to define the lag-response association, the results were largely the same (Figs. S19, S20). The most notable change for both sensitivity analyses was observed in the lag-response associations, with a slight change in the day-to-day variability in risk across the lag interval. When defining the cubic spline for the exposure–response association, once knots were placed at both the 75th and 90th percentiles, the results were insensitive to knot placement (Fig. S21). However, if knots at the 75th or 90th percentile were removed, there was an attenuation of the effect measures, demonstrating the importance of knot placement. Finally, when daily mean apparent temperature or daily maximum ambient temperature was used as the exposure of interest instead of daily mean ambient temperature, there was no notable change in the exposure-lag-response associations (Fig. S22).

4. Discussion

Across the 120 MSAs, extreme heat significantly increased the risk of CVD hospitalization among older urban populations by approximately 1.5%. The observed risk was driven by associations 3–10 days prior to CVD hospitalization, indicating that extreme heat may pose a delayed threat to cardiovascular morbidity. This increased risk led to a notable heat-attributable burden of over 37,000 CVD hospitalizations during the 18-year study period. Using the average payment due to provider (approximately $8,910), we can estimate that the heat-related economic burden of CVD hospitalizations for Medicare enrollees between 2000 and 2017 was $329.9 million. There were also differences by subpopulation, where black, female, and older individuals, those with CKD, and those with diabetes had a moderately higher extreme heat-related risk, resulting in 10,000–19,000 more heat-attributable CVD admissions than their counterparts. These groups also tended to have slightly lower MHPs, steeper risk curves, and more immediate responses at high temperatures, indicating a potentially lower heat tolerance.

When considering the role of UHIs, we observed a notably higher heat-related CVD burden in areas with higher surface UHII, attributed to moderately higher extreme heat-related risk. More specifically, high UHII areas, compared with low UHII areas, had a 1.4% higher CVD hospitalization risk associated with extreme heat and upwards of 11,000 more heat-attributable CVD admissions, accounting for over one-third of the total heat-attributable CVD burden. In terms of the billing costs, the estimated heat-related CVD economic burden in high UHII areas was $114.4 million (approximately $132,400 per 100,000 beneficiaries annually), compared to $12.7 million in low UHII areas (approximately $11,900 per 100,000 beneficiaries annually).

High UHII also had a disproportionate impact on already heat-vulnerable populations. Among the most heat-vulnerable enrollees (those who were black, female, older, had CKD, or had diabetes), the extreme heat-related CVD hospitalization risk in high UHII areas exceeded that in low UHII areas by 1.1–3.1%, with 8–33 more heat-attributable CVD admissions per 100,000 beneficiaries each year. In the less vulnerable subpopulations, the RR and AR were only 0.0–1.0% and 4–12 admissions higher. Across all the analyses, the

populations most at-risk of and burdened by extreme heat were females, individuals aged 75–114, those with CKD, and those with diabetes living in high UHII areas.

The observed differences in the heat-related CVD impacts between high and low UHII areas are likely due to several factors, including differences in exposure, vulnerability, and susceptibility. First, the interpolated weather station data used in this study likely does not capture the fine-scale spatial gradients in temperature associated with localized UHIs. This could, in part, be due to weather stations being located outside the urban cores and may explain why high and low UHII areas on average had similar ambient temperatures (Table 1). Because the UHII metric was based on fine-resolution satellite data, it may be able to better distinguish temperature changes over shorter distances. Though surface UHII is not a direct measure of heat exposure, the larger impacts observed in UHI-affected areas may be due to the high UHII category identifying areas that are on average exposed to higher air temperatures. Air temperatures and LSTs are often correlated (Schwarz et al., 2012) and urban cores with higher surface UHII are expected to also have higher air temperatures (Chakraborty et al., 2020). Additionally, air temperatures in high UHII areas may be experienced differently, as heavily urbanized areas often have less greenspace, limited shade, and absorb more solar radiation, all of which can decrease thermal comfort (Jamei et al., 2016).

Further, communities with high coverage of air conditioning (AC), trees, or well-insulated homes, and those more willing or able to change behavior during warm weather, may be less vulnerable to heat (Lane et al., 2014; Samuelson et al., 2020). UHI-affected areas tend to have lower access to AC (Romitti et al., 2022) and other adaptation resources (Palinkas et al., 2022) and are often home to already disadvantaged, heat-vulnerable groups, such low-income communities or people of color (Benz and Burney, 2021; Hsu et al., 2021; Johnson, 2022; Manware et al., 2022). Individuals in low-income communities are also more likely work outdoors or in facilities lacking AC (Gubernot et al., 2014). In this study, high UHII areas were generally of lower socioeconomic status, more racially diverse, and had less greenspace (Table S5, Fig. S23). These social and economic disadvantages combined may limit UHI-affected communities' ability to mitigate heat exposure, putting them at an elevated risk during extreme heat events (O'Lenick et al., 2020). Further, the reliability of a city's infrastructure and utilities during extreme weather may also play a role. For example, if part of a metropolitan area experiences electrical grid failures during a heat wave, this could increase the vulnerability of that specific population (Sailor et al., 2019; Stone et al., 2021). Taken together, the above factors may explain why people living in areas with UHIs likely experience greater heat-related CVD impacts.

Although heat increased the risk and burden of CVD hospitalizations across the contiguous US and in high UHII areas, there was considerable variation at the MSA level. While two-thirds of MSAs had an overall increased CVD risk or burden associated with extreme heat, only about half had larger heat-related CVD impacts in high UHII areas compared to low UHII areas. This city-to-city variation is likely due to many of the same factors discussed above. It may also be due to spatiotemporal changes in heat vulnerability and adaptation (Sheridan and Dixon, 2017), differences in heat acclimatization due to a combination of physiological, behavioral, and environmental factors (Hanna and Tait, 2015), variation

in the associations between heat and mortality (Phung et al., 2016), or differences in the demographic composition across cities. The lack of striking geographic, regional, or climactic trends in the MSAs at highest risk, overall and by UHII level, indicate that regional climate may not be the most important factor when determining vulnerability. Geographic variability in heat-related morbidity is consistent with previous findings (Gasparrini et al., 2015; Gronlund et al., 2014; Scovronick et al., 2018; Yang et al., 2015) and may suggest that city-specific mitigation and adaptation strategies are needed to address intensifying UHIs and rising temperatures.

Across all analyses, the oldest enrollees had the highest risk of heat-related CVD hospitalization. Older adults are likely more heat-vulnerable because ageing can impair the physiological response to heat (Meade et al., 2020). However, given the distribution of CVD hospitalizations across age groups within other subpopulations (Table S6), age was likely not the primary driver of the observed differences in risk by sex, race, and chronic conditions. For example, individuals with diabetes and CKD are often more susceptible in warm weather because they have poorer thermoregulation (Petrofsky, 2011) and increased dehydration risk (Lee et al., 2019), respectively. Individuals with chronic conditions also frequently use medications that can increase heat sensitivity (Layton et al., 2020). Females likely have an increased risk of heat-related cardiovascular morbidity due to a combination of biological factors, such as a lower capacity for vasodilatation and perspiration, and social factors, including being more likely to live alone (van Steen et al., 2019). The elevated risk among black enrollees is probably due in part to social factors, including having lower income, limited AC access, and higher rates of pre-existing conditions, that result from structural racism and discriminatory policies (Bailey et al., 2017; Hoffman et al., 2020). UHIs further elevating the CVD risk and burden among these already vulnerable populations is likely caused by the combination of these socioeconomic, biological, and environmental factors which make certain areas and populations more vulnerable and susceptible to heat. This compounding risk emphasizes the differential impact of extreme heat and UHIs and is important to account for when identifying the most heat-vulnerable communities and developing context-specific heat preparation and response plans. Additionally, future work evaluating how heat-related CVD risk and burden varies by other demographic characteristics within each subpopulation may be valuable for further pinpointing who is most heat vulnerable.

Existing literature can provide additional context for the findings presented. First, many previous epidemiologic studies have also observed an increased risk of CVD hospitalization following exposure to high temperatures or a heat wave (Chen et al., 2019; Lam et al., 2018; Li et al., 2019; Lin et al., 2009; Liu et al., 2018; Son et al., 2014; Wang et al., 2022, 2021; Zhao et al., 2018b). Some similarly found the MHP or MHT to be located at or above the 90th temperature percentile (Bai et al., 2018; Lam et al., 2018) or around 25 °C (Lu et al., 2020). Others likewise observed a slightly delayed response, with the greatest risk between 2 and 6 days after exposure (Li et al., 2019; Lin et al., 2009; Wang et al., 2022; Zhao et al., 2018b). Further, previous work has similarly identified an increased heat-related morbidity and mortality risk in older adults (Cui et al., 2019; Lin et al., 2009; Wang et al., 2021), females (Bai et al., 2018; Cui et al., 2019; Li et al., 2019; Song et al., 2017; Wang et al., 2022), black individuals (Gronlund, 2014), and those with diabetes (Chen et

al., 2019; Lam et al., 2018). Of the few studies that have considered the health impact of UHIs, many have identified a higher mortality risk (Goggins et al., 2012; Taylor et al., 2015) and burden (Dang et al., 2018; Heaviside et al., 2016; Huang et al., 2020) in these areas. Others found that areas with lower greenspace, which can be used as a proxy for UHIs, have an increased risk of heat-related morbidity and mortality (Choi et al., 2022; Gronlund et al., 2015; Henderson et al., 2022; Madrigano et al., 2013; Morais et al., 2021; Zhang et al., 2021). However, greenspace is not always a reliable indicator of UHIs in more arid climates, such as the southwestern US (Fig. S24), highlighting the necessity of UHI-specific analyses.

This study has several strengths that distinguish it from previous works. First, the size of the dataset, totaling to over 48 million CVD hospitalizations across 18 years in 120 different urban areas, is much larger than those previously used in epidemiologic studies on heat-related cardiovascular morbidity, many of which relied on data from only a single city (Cui et al., 2019; Guo et al., 2017; Wang et al., 2021, 2022). Second, this larger dataset allowed for the consideration of risk modification by comorbidities and race, subpopulations which have been historically overlooked due to insufficient data. We also analyzed associations across multiple US cities, providing valuable insight into the city-to-city variation in heat-related cardiovascular morbidity risk and burden. Third, ZIP code-level exposure and outcome data were used, which is a smaller spatial resolution than the city-level data used in many prior studies (Cui et al., 2019; Guo et al., 2017; Iñiguez et al., 2021; Martinez-Solanas and Basagana, 2019; Wang et al., 2021) and allowed for an investigation into how associations differed between areas with and without UHIs within each metropolitan area. These ZIP code-level data, in combination with the population weighting approach, likely provided more informed estimates of population-level exposure. Finally, this study used a direct measure of UHII to characterize UHIs, instead of relying on measures like greenspace as a proxy. This measure of UHII has been shown to be relatively accurate (Chakraborty and Lee, 2019) and allowed for identification of differences in heat-related cardiovascular morbidity impacts between areas affected and unaffected by UHIs.

There are also important limitations that must be considered. First, because measurements of individual-level exposure to ambient temperature and surface UHII were unavailable, there is the possibility of exposure misclassification. However, any misclassification would likely be nondifferential, attenuating the results towards the null. Additionally, the weather station data may have not been finely resolved enough to capture ambient temperature differences across an urban core. It may be valuable to investigate these associations using temperature data at a finer spatial scale. Second, because the UHII metric was only available for a single, averaged time period, we were unable to account for changes in UHIs over time. Additionally, there may be limitations with the UHII metric itself, given that it is a clear sky estimate for 2013–2017, with cloudy days excluded, and not necessarily representative of the average state during the entire 18-year study period. Given increasing urbanization in the US (Bounoua et al., 2018), future research should evaluate if the expansion and intensification of UHIs over time influence their role in heat-related cardiovascular morbidity. Further, the US-wide categorization of UHII meant that some MSAs did not have any ZIP codes categorized as high UHII. It may be valuable for future work to investigate the impacts of UHIs using a relative measure with an MSA-specific categorization of UHII. Third, the subpopulation counts by race only included black and

white enrollees due to insufficient hospitalization counts in other categories. Future studies with larger datasets might provide assessments for other groups. This analysis also did not consider specific CVD subtypes, which should be considered in future work. Fourth, it was not possible to account for all potentially relevant ZIP code-level factors, such as AC coverage or precipitation, due to lack of data or limited spatial detail in the data available. Because housing and environment characteristics likely play an important role in the observed associations, this should be considered in future research. Fifth, the MHP was defined using the pooled association to maximize information and minimize bias. However, it may not always correspond with the minimum point on an MSA-specific curve and may be worth-while to investigate if the MHP varies geographically. Sixth, the 95% CIs around the burden estimates may be artificially small given that they did not account for uncertainty in the temperature estimates (Cleland et al., 2021). Additionally, the burden estimates likely underestimate the total heat-attributable burden as they only accounted for CVD impacts in the urban Medicare population that resulted in hospitalization. Finally, we did not test for significant differences in RR between low and high UHII areas and subpopulations. Therefore, the observed differences may not be statistically significant but are indicative of potential differences that warrant further investigation.

To identify opportunities for intervention and ensure the most at-risk communities can be protected during extreme heat events moving forward, future work should aim to identify the socioeconomic and environmental drivers of the observed differences between MSAs, subpopulations, and low and high UHII areas. Additionally, the vulnerability of UHI-affected communities and the heat-attributable CVD burden in US cities are likely to increase with increasing temperatures. As such, estimates of the future burden of heat-related cardiovascular morbidity, both inside and outside of UHI-affected areas, should take into consideration climate change, urbanization, and an ageing, growing population. To do this, it would be valuable to evaluate if the UHII- and subpopulation-specific risk has changed over time, especially given evidence of recent decreases in heat vulnerability (Sheridan and Allen, 2018). Research into the cardiovascular impacts of other extreme heat metrics, such as prolonged periods of high temperatures, may also be informative given the expected increase in the frequency, intensity, and duration of heat waves. Finally, additional research considering the combined impact of heat and UHIs on different health outcomes, among multiple subpopulations, and in different parts of the world is needed to corroborate our results and further explore how the health and wellbeing of urban populations will be impacted by climate change.

5. Conclusions

This study illuminates the impact of extreme heat exposure on cardiovascular morbidity among older adults living in areas experiencing UHIs across the US. This is the first multi-city analysis to suggest that surface UHIs may elevate the risk and burden of heat-related CVD hospitalizations and demonstrate that not all cities are equally impacted by heat nor UHIs. It is also the first to identify a more pronounced impact of UHIs in already heat-vulnerable populations, revealing a disproportionate heat vulnerability for females, individuals over 75, those with diabetes, and those with CKD living in UHI-affected communities.

Supplementary Material

Refer to Web version on PubMed Central for supplementary material.

Funding

Data statement

The ZIP code-level daily temperature and relative humidity data can be downloaded at: https://doi.org/10.15139/S3/ZL4UF9. The code and data for the interactive dashboard can be viewed at: https://github.com/stephcleland/Heat-CVD-UHI-Dashboard. The authors do not have permission to share the Medicare data.

Data availability

Download ZIP code-level weather data at: https://doi.org/10.15139/S3/ZL4UF9. View interactive dashboard code at: https://github.com/stephcleland/Heat-CVD-UHI-Dashboard. Authors are unable to share Medicare data.

Abbreviations:

UHII	Urban Heat Island Intensity
CVD	Cardiovascular Disease
MSA	Metropolitan Statistical Area
CI	Confidence Interval
UHI	Urban Heat Island
RH	Relative Humidity
US	United States
DLNM	Distributed Lag Non-linear Model
OMB	Office of Management and Budget
ICD-9	International Classification of Diseases, Ninth Revision
ICD-10	International Classification of Diseases, Tenth Revision
CKD	Chronic Kidney Disease
RR	Relative Risk
AN	Attributable Number

AF	Attributable Fraction
AR	Attributable Rate
LST	Land Surface Temperature
MODIS	Moderate Resolution Imaging Spectroradiometer
MHP	Minimum Hospitalization Percentile
MHT	Minimum Hospitalization Temperature
IQR	Interquartile Range
AC	Air Conditioning
df	Degrees of Freedom

References

Åström DO, Bertil F, Joacim R, 2011. Heat wave impact on morbidity and mortality in the elderly population: A review of recent studies. Maturitas 69, 99–105. 10.1016/J.MATURITAS.2011.03.008. [PubMed: 21477954]

Bai L, Li Q, Wang J, Lavigne E, Gasparrini A, Copes R, Yagouti A, Burnett RT, Goldberg MS, Cakmak S, Chen H, 2018. Increased coronary heart disease and stroke hospitalisations from ambient temperatures in Ontario. Heart 104, 673–679. 10.1136/HEARTJNL-2017-311821. [PubMed: 29101264]

Bai L, Li Q, Wang J, Lavigne E, Gasparrini A, Copes R, Yagouti A, Burnett RT, Goldberg MS, Villeneuve PJ, Cakmak S, Chen H, 2016. Hospitalizations from Hypertensive Diseases, Diabetes, and Arrhythmia in Relation to Low and High Temperatures: Population-Based Study. Sci. Rep 6, 1–9. 10.1038/srep30283. [PubMed: 28442746]

Bailey ZD, Krieger N, Agénor M, Graves J, Linos N, Bassett MT, 2017. Structural racism and health inequities in the USA: evidence and interventions. Lancet (London, England) 389, 1453–1463. 10.1016/S0140-6736(17)30569-X. [PubMed: 28402827]

Benz SA, Burney JA, 2021. Widespread Race and Class Disparities in Surface Urban Heat Extremes Across the United States. Earth's Futur. 9.

Boersma P, Black LI, Ward BW, 2020. Prevalence of multiple chronic conditions among US adults, 2018. Prev. Chronic Dis 17 10.5888/PCD17.200130.

Bounoua L, Nigro J, Zhang P, Thome K, Lachir A, 2018. Mapping urbanization in the United States from 2001 to 2011. Appl. Geogr 90, 123–133. 10.1016/j.apgeog.2017.12.002.

Bunker A, Wildenhain J, Vandenbergh A, Henschke N, Rocklöv J, Hajat S, Sauerborn R, 2016. Effects of Air Temperature on Climate-Sensitive Mortality and Morbidity Outcomes in the Elderly; a Systematic Review and Meta-analysis of Epidemiological Evidence. EBioMedicine 6, 258–268. 10.1016/j.ebiom.2016.02.034. [PubMed: 27211569]

Burkart K, Meier F, Schneider A, Breitner S, Canário P, Alcoforado MJ, Scherer D, Endlicher W, 2016. Modification of heat-related mortality in an elderly urban population by vegetation (Urban green) and proximity to water (Urban blue): Evidence from Lisbon. Portugal. Environ. Health Perspect 124, 927–934. 10.1289/ehp.1409529. [PubMed: 26566198]

Chakraborty T, Hsu A, Manya D, Sheriff G, 2020. A spatially explicit surface urban heat island database for the United States: Characterization, uncertainties, and possible applications. ISPRS J. Photogramm. Remote Sens 168, 74–88. 10.1016/j.isprsjprs.2020.07.021.

Chakraborty T, Lee X, 2019. A simplified urban-extent algorithm to characterize surface urban heat islands on a global scale and examine vegetation control on their spatiotemporal variability. Int. J. Appl. Earth Obs. Geoinf 74, 269–280. 10.1016/j.jag.2018.09.015.

Chen K, Breitner S, Wolf K, Hampel R, Meisinger C, Heier M, Von Scheidt W, Kuch B, Peters A, Schneider A, Schulz H, Schwettmann L, Leidl R, Strauch K, 2019. Temporal variations in the triggering of myocardial infarction by air temperature in Augsburg, Germany, 1987–2014. Eur. Heart J 40, 1600–1608. 10.1093/EURHEARTJ/EHZ116. [PubMed: 30859207]

Choi HM, Lee W, Roye D, Heo S, Urban AS, Entezari A, Vicedo-Cabrera AM, Zanobetti A, Gasparrini A, Analitis A, Tobias A, Armstrong B, Forsberg B, I~ Niguez C, Str€Om CA, Indermitte E, Lavigne E, Mayvaneh F, Acquaotta F, Sera F, Orru H, Kim H, Kysel J, Madueira J, Schwartz J, Jaakkola JJK, Katsouyanni K, Hurtado Diaz M, Ragettli MS, Pascal M, Ryti N, Scovronick N, Osorio S, Tong S, Seposo X, Guo YYL, Guo YYL, Bell ML, Choi HM, 2022. Effect modification of greenness on the association between heat and mortality: A multi-city multi-country study. eBioMedicine 84, 104251. 10.1016/J.EBIOM.2022.104251. [PubMed: 36088684]

Cicci KR, Maltby A, Clemens KK, Vicedo-Cabrera AM, Gunz AC, Lavigne É, Wilk P, 2022. High Temperatures and Cardiovascular-Related Morbidity: A Scoping Review. Int. J. Environ. Res. Public Health 19, 11243. 10.3390/ijerph191811243. [PubMed: 36141512]

Cleland SE, Serre ML, Rappold AG, West JJ, 2021. Estimating the Acute Health Impacts of Fire-Originated PM2.5 Exposure During the 2017 California Wildfires: Sensitivity to Choices of Inputs. GeoHealth 5. 10.1029/2021GH000414.

Cromartie J, 2018. Rural America at a Glance, 2018 Edition, Economic Information Bulletin.

Cui L, Geng X, Ding T, Tang J, Xu J, Zhai J, 2019. Impact of ambient temperature on hospital admissions for cardiovascular disease in Hefei City. China. Int. J. Biometeorol 63, 723–734. 10.1007/s00484-019-01687-0. [PubMed: 30852664]

Dang TN, Van DQ, Kusaka H, Seposo XT, Honda Y, 2018. Green Space and Deaths Attributable to the Urban Heat Island Effect in Ho Chi Minh City. Am. J. Public Health 108, S137–S143. 10.2105/AJPH.2017.304123. [PubMed: 29072938]

Gasparrini A, 2014. Modeling exposure-lag-response associations with distributed lag non-linear models. Stat. Med 33, 881–899. 10.1002/sim.5963. [PubMed: 24027094]

Gasparrini A, 2011. Distributed lag linear and non-linear models in R: The package dlnm. J. Stat. Softw 43, 2–20. 10.18637/jss.v043.i08.

Gasparrini A, Armstrong B, Kenward MG, 2012. Multivariate meta-analysis for non-linear and other multi-parameter associations. Stat. Med 31, 3821–3839. 10.1002/sim.5471. [PubMed: 22807043]

Gasparrini A, Guo Y, Hashizume M, 2015. Mortality risk attributable to high and low ambient temperature: a multicountry observational study. Lancet 386, 369–375. 10.1016/S0140-6736(14)62114-0. [PubMed: 26003380]

Gasparrini A, Leone M, 2014. Attributable risk from distributed lag models. BMC Med. Res. Methodol 14, 1–8. 10.1186/1471-2288-14-55. [PubMed: 24383436]

Goggins WB, Chan EYY, Ng E, Ren C, Chen L, 2012. Effect modification of the association between short-term meteorological factors and mortality by urban heat islands in Hong Kong. PLoS One 7, e38551. [PubMed: 22761684]

Gostimirovic M, Novakovic R, Rajkovic J, Djokic V, Terzic D, Putnik S, Gojkovic-Bukarica L, 2020. The influence of climate change on human cardiovascular function. Arch. Environ. Occup. Heal 75, 406–414. 10.1080/19338244.2020.1742079.

Green H, Bailey J, Schwarz L, Vanos J, Ebi K, Benmarhnia T, 2019. Impact of heat on mortality and morbidity in low and middle income countries: A review of the epidemiological evidence and considerations for future research. Environ. Res 10.1016/j.envres.2019.01.010.

Gronlund CJ, 2014. Racial and Socioeconomic Disparities in Heat-Related Health Effects and Their Mechanisms: a Review. Curr. Epidemiol. Reports 1, 165–173. 10.1007/s40471-014-0014-4.

Gronlund CJ, Berrocal VJ, White-Newsome JL, Conlon KC, O'Neill MS, 2015. Vulnerability to extreme heat by socio-demographic characteristics and area green space among the elderly in Michigan, 1990–2007. Environ. Res 136, 449–461. 10.1016/j.envres.2014.08.042. [PubMed: 25460667]

Gronlund CJ, Zanobetti A, Schwartz JD, Wellenius GA, O'Neill MS, 2014. Heat, heat waves, and hospital admissions among the elderly in the United States, 1992–2006. Environ. Health Perspect 122, 1187–1192. 10.1289/ehp.1206132. [PubMed: 24905551]

Gronlund CJ, Zanobetti A, Wellenius GA, Schwartz JD, O'Neill MS, 2016. Vulnerability to renal, heat and respiratory hospitalizations during extreme heat among U.S. elderly. Clim. Change 136, 631–645. 10.1007/s10584-016-1638-9. [PubMed: 27453614]

Gubernot DM, Anderson GB, Hunting KL, 2014. The epidemiology of occupational heat exposure in the United States: a review of the literature and assessment of research needs in a changing climate. Int. J. Biometeorol 58, 1779–1788. 10.1007/s00484-013-0752-x. [PubMed: 24326903]

Guo P, Zheng M, Feng W, Wu J, Deng C, Luo G, Wang L, Pan B, Liu H, 2017. Effects of ambient temperature on stroke hospital admissions: Results from a time-series analysis of 104,432 strokes in Guangzhou. China. Sci. Total Environ 580, 307–315. 10.1016/J.SCITOTENV.2016.11.093. [PubMed: 28011022]

Hanna EG, Tait PW, 2015. Limitations to thermoregulation and acclimatization challenge human adaptation to global warming. Int. J. Environ. Res. Public Health 12, 8034–8074. 10.3390/ijerph120708034. [PubMed: 26184272]

Heaviside C, Macintyre H, Vardoulakis S, 2017. The Urban Heat Island: Implications for Health in a Changing Environment. Curr. Environ. Heal. Reports 4, 296–305. 10.1007/s40572-017-0150-3.

Heaviside C, Vardoulakis S, Cai XM, 2016. Attribution of mortality to the urban heat island during heatwaves in the West Midlands. UK. Environ. Heal 15, 49–59. 10.1186/s12940-016-0100-9.

Henderson SB, McLean KE, Lee MJ, Kosatsky T, 2022. Analysis of community deaths during the catastrophic 2021 heat dome. Environ. Epidemiol 6, E189. 10.1097/EE9.0000000000000189. [PubMed: 35169667]

Heo S, Chen C, Kim H, Sabath B, Dominici F, Warren JL, Di Q, Schwartz J, Bell ML, 2021. Temporal changes in associations between high temperature and hospitalizations by greenspace: Analysis in the Medicare population in 40 U.S. northeast counties. Environ. Int 156, 106737 10.1016/j.envint.2021.106737. [PubMed: 34218185]

Ho JY, Shi Y, Lau KKL, Ng EYY, Ren C, Goggins WB, 2023. Urban heat island effect-related mortality under extreme heat and non-extreme heat scenarios: A 2010–2019 case study in Hong Kong. Sci. Total Environ 858, 159791 10.1016/J.SCITOTENV.2022.159791. [PubMed: 36328261]

Hoffman JS, Shandas V, Pendleton N, 2020. The Effects of Historical Housing Policies on Resident Exposure to Intra-Urban Heat: A Study of 108 US Urban Areas. Clim. 2020, Vol. 8, Page 12 8, 12. 10.3390/CLI8010012.

Hondula DM, Davis RE, Leisten MJ, Saha MV, Veazey LM, Wegner CR, 2012. Fine-scale spatial variability of heat-related mortality in Philadelphia County, USA, from 1983–2008: A case-series analysis. Environ. Heal. A Glob. Access Sci. Source 11, 1–11. 10.1186/1476-069X-11-16.

Hsu A, Sheriff G, Chakraborty T, Manya D, 2021. Disproportionate exposure to urban heat island intensity across major US cities. Nat. Commun 12, 1–11. 10.1038/s41467-021-22799-5. [PubMed: 33397941]

Huang H, Deng X, Yang H, Zhou X, Jia Q, 2020. Spatio-Temporal Mechanism Underlying the Effect of Urban Heat Island on Cardiovascular Diseases. Iran. J. Public Health 49.

Huang K, Li X, Liu X, Seto KC, 2019. Projecting global urban land expansion and heat island intensification through 2050. Environ. Res. Lett 14, 114037 10.1088/1748-9326/ab4b71.

Hurtado-Díaz M, Cruz JC, Texcalac-Sangrador JL, Félix-Arellano EE, Gutíerrez-Ávila I, Briseño-Pérez AA, Saavedra-Lara N, Tobías A, Riojas-Rodríguez H, 2019. Short-term effects of ambient temperature on non-external and cardiovascular mortality among older adults of metropolitan areas of Mexico. Int. J. Biometeorol 63, 1641–1650. 10.1007/s00484-019-01778-y. [PubMed: 31407098]

Iñiguez C, Roýe D, Tobías A, 2021. Contrasting patterns of temperature related mortality and hospitalization by cardiovascular and respiratory diseases in 52 Spanish cities. Environ. Res 192, 110191 10.1016/J.ENVRES.2020.110191. [PubMed: 32980302]

Jamei E, Rajagopalan P, Seyedmahmoudian M, Jamei Y, 2016. Review on the impact of urban geometry and pedestrian level greening on outdoor thermal comfort. Renew. Sustain. Energy Rev 54, 1002–1017. 10.1016/J.RSER.2015.10.104.

Johnson DP, 2022. Population-Based Disparities in U.S. Urban Heat Exposure from 2003 to 2018. Int. J. Environ. Res. Public Health 19, 12314. 10.3390/IJERPH191912314. [PubMed: 36231614]

Johnson RJ, Sánchez-Lozada LG, Newman LS, Lanaspa MA, Diaz HF, Lemery J, Rodriguez-Iturbe B, Tolan DR, Butler-Dawson J, Sato Y, Garcia G, Hernando AA, Roncal-Jimenez CA, 2019. Climate Change and the Kidney. Ann. Nutr. Metab 74, 38–44. 10.1159/000500344. [PubMed: 31203298]

Lam HCY, Chan JCN, Luk AOY, Chan EYY, Goggins WB, 2018. Short-term association between ambient temperature and acute myocardial infarction hospitalizations for diabetes mellitus patients: A time series study. PLoS Med. 15, e1002612. [PubMed: 30016318]

Lane K, Wheeler K, Charles-Guzman K, Ahmed M, Blum M, Gregory K, Graber N, Clark N, Matte T, 2014. Extreme heat awareness and protective behaviors in New York City. J. Urban Heal 91, 403–414. 10.1007/s11524-013-9850-7.

Layton JB, Li W, Yuan J, Gilman JP, Horton DB, Setoguchi S, 2020. Heatwaves, medications, and heat-related hospitalization in older Medicare beneficiaries with chronic conditions. PLoS One 15. 10.1371/journal.pone.0243665.

Lee WS, Kim WS, Lim YH, Hong YC, 2019. High temperatures and kidney disease morbidity: A Systematic Review and Meta-analysis. J. Prev. Med. Public Heal 52, 1–13. 10.3961/jpmph.18.149.

Li M, Shaw BA, Zhang W, Vásquez E, Lin S, 2019. Impact of Extremely Hot Days on Emergency Department Visits for Cardiovascular Disease among Older Adults in New York State. Int. J. Environ. Res. Public Health 16, 2119. 10.3390/ijerph16122119. [PubMed: 31207990]

Lin S, Luo M, Walker RJ, Liu X, Hwang SA, Chinery R, 2009. Extreme high temperatures and hospital admissions for respiratory and cardiovascular diseases. Epidemiology 20, 738–746. 10.1097/EDE.0B013E3181AD5522. [PubMed: 19593155]

Liu Y, Hoppe BO, Convertino M, 2018. Threshold Evaluation of Emergency Risk Communication for Health Risks Related to Hazardous Ambient Temperature. Risk Anal. 38, 2208–2221. 10.1111/RISA.12998. [PubMed: 29637591]

Lu P, Xia G, Zhao Q, Xu R, Li S, Guo Y, 2020. Temporal trends of the association between ambient temperature and hospitalisations for cardiovascular diseases in Queensland, Australia from 1995 to 2016: A time-stratified case-crossover study. PLoS Med. 17, e1003176. [PubMed: 32692738]

Macintyre HL, Heaviside C, Taylor J, Picetti R, Symonds P, Cai XM, Vardoulakis S, 2018. Assessing urban population vulnerability and environmental risks across an urban area during heatwaves – Implications for health protection. Sci. Total Environ 610–611, 678–690. 10.1016/j.scitotenv.2017.08.062.

Madrigano J, Mittleman MA, Baccarelli A, Goldberg R, Melly S, Von Klot S, Schwartz J, 2013. Temperature, myocardial infarction, and mortality: Effect modification by individual-and area-level characteristics. Epidemiology 24, 439–446. 10.1097/EDE.0b013e3182878397. [PubMed: 23462524]

Manware M, Dubrow R, Carrión D, Ma Y, Chen K, 2022. Residential and Race/Ethnicity Disparities in Heat Vulnerability in the United States. GeoHealth 6.

Martinez-Solanas E, Basagana X, 2019. Temporal changes in the effects of ambient temperatures on hospital admissions in Spain. PLoS One 14, e0218262. [PubMed: 31194811]

Martínez-Solanas É, Quijal-Zamorano M, Achebak H, Petrova D, Robine JM, Herrmann FR, Rodó X, Ballester J, 2021. Projections of temperature-attributable mortality in Europe: a time series analysis of 147 contiguous regions in 16 countries. Lancet Planet. Heal 5, e446–e454. 10.1016/S2542-5196(21)00150-9.

Meade RD, Akerman AP, Notley SR, McGinn R, Poirier P, Gosselin P, Kenny GP, 2020. Physiological factors characterizing heat-vulnerable older adults: A narrative review. Environ. Int 144, 105909 10.1016/j.envint.2020.105909. [PubMed: 32919284]

Milojevic A, Armstrong BG, Gasparrini A, Bohnenstengel SI, Barratt B, Wilkinson P, 2016. Methods to Estimate Acclimatization to Urban Heat Island Effects on Heat- and Cold-Related Mortality. Environ. Health Perspect 124, 1016–1022. 10.1289/EHP.1510109. [PubMed: 26859738]

Mistry MN, Schneider R, Masselot P, Roýe D, Armstrong B, Kyselý J, Orru H, Sera F, Tong S, Lavigne É, Urban A, Madureira J, García-Leòn D, Ibarreta D, Ciscar JC, Feyen L, de Schrijver E, de Sousa Zanotti Stagliorio Coelho M, Pascal M, Tobias A, Alahmad B, Abrutzky R, Saldiva PHN, Correa PM, Orteg NV, Kan H, Osorio S, Indermitte E, Jaakkola JJK, Ryti N, Schneider A, Huber V, Katsouyanni K, Analitis A, Entezari A, Mayvaneh F, Michelozzi P, De'Donato F, Hashizume M, Kim Y, Diaz MH, De la Cruz Valencia C, Overcenco A, Houthuijs D, Ameling

C, Rao S, Seposo X, Nunes B, Holobaca IH, Kim H, Lee W, Íñiguez C, Forsberg B, Åström C, Ragettli MS, Guo YYLL, Chen BY, Colistro V, Zanobetti A, Schwartz J, Dang TN, Van Dung D, Guo YYLL, Vicedo-Cabrera AM, Gasparrini A, 2022. Comparison of weather station and climate reanalysis data for modelling temperature-related mortality. Sci. Rep 12, 1–14. 10.1038/ s41598-022-09049-4. [PubMed: 34992227]

Mohajerani A, Bakaric J, Jeffrey-Bailey T, 2017. The urban heat island effect, its causes, and mitigation, with reference to the thermal properties of asphalt concrete. J. Environ. Manage 197, 522–538. 10.1016/j.jenvman.2017.03.095. [PubMed: 28412623]

Mora C, Dousset B, Caldwell IR, Powell FE, Geronimo RC, Bielecki CR, Counsell CWW, Dietrich BS, Johnston ET, Louis LV, Lucas MP, Mckenzie MM, Shea AG, Tseng H, Giambelluca TW, Leon LR, Hawkins E, Trauernicht C, 2017. Global risk of deadly heat. Nat. Clim. Chang 7, 501–506. 10.1038/nclimate3322.

Morais L, Lopes A, Nogueira P, 2021. Human health outcomes at the neighbourhood scale implications: Elderly's heat-related cardiorespiratory mortality and its influencing factors. Sci. Total Environ 760, 144036 10.1016/j.scitotenv.2020.144036. [PubMed: 33348162]

Oceanic, N., Administration, A., 2022. Global Surface Summary of the Day. Natl. Clim, Data Cent https://www.ncei.noaa.gov/access/search/data-search/global-summary-of-the-day (accessed 10.7.22.

O'Lenick CR, Baniassadi A, Michael R, Monaghan A, Boehnert J, Yu X, Hayden MH, Wiedinmyer C, Zhang K, Crank PJ, Heusinger J, Hoel P, Sailor DJ, Wilhelmi OV, 2020. A case-crossover analysis of indoor heat exposure on mortality and hospitalizations among the elderly in Houston. Texas. Environ. Health Perspect 128, 1–17. 10.1289/EHP6340.

Oke TR, Mills G, Christen A, Voogt JA, 2017. Urban climates. Cambridge University Press. 10.1017/9781139016476.

Palinkas LA, Hurlburt MS, Fernandez C, De Leon J, Yu K, Salinas E, Garcia E, Johnston J, Rahman MM, Silva SJ, McConnell RS, 2022. Vulnerable, Resilient, or Both? A Qualitative Study of Adaptation Resources and Behaviors to Heat Waves and Health Outcomes of Low-Income Residents of Urban Heat Islands. Int. J. Environ. Res. Public Health 19, 11090. 10.3390/ IJERPH191711090/S1. [PubMed: 36078804]

Petrofsky JS, 2011. The effect of type-2-diabetes-related vascular endothelial dysfunction on skin physiology and activities of daily living. J. Diabetes Sci. Technol 5, 657–667. 10.1177/193229681100500319. [PubMed: 21722580]

Phung D, Thai PK, Guo Y, Morawska L, Rutherford S, Chu C, 2016. Ambient temperature and risk of cardiovascular hospitalization: An updated systematic review and meta-analysis. Sci. Total Environ 550, 1084–1102. 10.1016/J.SCITOTENV.2016.01.154. [PubMed: 26871555]

Rizwan AM, Dennis LYC, Liu C, 2008. A review on the generation, determination and mitigation of Urban Heat Island. J. Environ. Sci 20, 120–128. 10.1016/S1001-0742(08)60019-4.

Romitti Y, Sue Wing I, Spangler KR, Wellenius GA, 2022. Inequality in the availability of residential air conditioning across 115 US metropolitan areas. PNAS Nexus 1. 10.1093/pnasnexus/pgac210.

Sailor DJ, Baniassadi A, O'Lenick CR, Wilhelmi OV, 2019. The growing threat of heat disasters. Environ. Res. Lett 14, 054006 10.1088/1748-9326/ab0bb9.

Samuelson H, Baniassadi A, Lin A, Izaga González P, Brawley T, Narula T, 2020. Housing as a critical determinant of heat vulnerability and health. Sci. Total Environ 720, 137296 10.1016/ j.scitotenv.2020.137296. [PubMed: 32325550]

Schwarz N, Schlink U, Franck U, Großmann K, 2012. Relationship of land surface and air temperatures and its implications for quantifying urban heat island indicators—An application for the city of Leipzig (Germany). Ecol. Indic 18, 693–704. 10.1016/J.ECOLIND.2012.01.001.

Scovronick N, Sera F, Acquaotta F, Garzena D, Fratianni S, Wright CY, Gasparrini A, 2018. The association between ambient temperature and mortality in South Africa: A time-series analysis. Environ. Res 161, 229–235. 10.1016/j.envres.2017.11.001. [PubMed: 29161655]

Sheridan SC, Allen MJ, 2018. Temporal trends in human vulnerability to excessive heat. Environ. Res. Lett 13, 043001 10.1088/1748-9326/aab214.

Sheridan SC, Dixon PG, 2017. Spatiotemporal trends in human vulnerability and adaptation to heat across the United States. Anthropocene 20, 61–73. 10.1016/j.ancene.2016.10.001.

Son J-Y, Liu JC, Bell ML, 2019. Temperature-related mortality: a systematic review and investigation of effect modifiers. Environ. Res. Lett 14, 073004 10.1088/1748-9326/AB1CDB.

Son JY, Bell ML, Lee JT, 2014. The impact of heat, cold, and heat waves on hospital admissions in eight cities in Korea. Int. J. Biometeorol 58, 1893–1903. 10.1007/s00484-014-0791-y. [PubMed: 24445484]

Song X, Wang S, Hu Y, Yue M, Zhang T, Liu Y, Tian J, Shang K, 2017. Impact of ambient temperature on morbidity and mortality: An overview of reviews. Sci. Total Environ 586, 241–254. 10.1016/j.scitotenv.2017.01.212. [PubMed: 28187945]

Stone B, Mallen E, Rajput M, Gronlund CJ, Broadbent AM, Krayenhoff ES, Augenbroe G, O'Neill MS, Georgescu M, 2021. Compound Climate and Infrastructure Events: How Electrical Grid Failure Alters Heat Wave Risk. Environ. Sci. Technol 55, 6957–6964. 10.1021/acs.est.1c00024. [PubMed: 33930272]

Taylor J, Wilkinson P, Davies M, Armstrong B, Chalabi Z, Mavrogianni A, Symonds P, Oikonomou E, Bohnenstengel SI, 2015. Mapping the effects of urban heat island, housing, and age on excess heat-related mortality in London. Urban Clim. 14, 517–528. 10.1016/J.UCLIM.2015.08.001.

Tobías A, Armstrong B, Gasparrini A, 2017. Brief report: Investigating uncertainty in the minimum mortality temperature. Epidemiology 28, 72–76. 10.1097/EDE.0000000000000567. [PubMed: 27748681]

Tong S, Prior J, McGregor G, Shi X, Kinney P, 2021. Urban heat: An increasing threat to global health. BMJ 375. 10.1136/bmj.n2467.

Tuholske C, Caylor K, Funk C, Verdin A, Sweeney S, Grace K, Peterson P, Evans T, 2021. Global urban population exposure to extreme heat. Proc. Natl. Acad. Sci. U. S. A 118 10.1073/PNAS.2024792118.

Turner LR, Barnett AG, Connell D, Tong S, 2012. Ambient temperature and cardiorespiratory morbidity: A systematic review and meta-analysis. Epidemiology 23, 594–606. 10.1097/EDE.0b013e3182572795. [PubMed: 22531668]

United Nations Department of Economic and Social Affairs, 2018. 68% of the world population projected to live in urban areas by 2050, says UN. UN DESA.

US National Weather Service, 2022. Meteorological Conversions and Calculations - Heat Index Calculation. Weather Predict, Cent https://www.wpc.ncep.noaa.gov/html/heatindex.shtml (accessed 10.7.22.

Vallianou NG, Geladari EV, Kounatidis D, Geladari CV, Stratigou T, Dourakis SP, Andreadis EA, Dalamaga M, 2021. Diabetes mellitus in the era of climate change. Diabetes Metab. 47, 101205 10.1016/J.DIABET.2020.10.003. [PubMed: 33127474]

van Steen Y, Ntarladima AM, Grobbee R, Karssenberg D, Vaartjes I, 2019. Sex differences in mortality after heat waves: are elderly women at higher risk? Int. Arch. Occup. Environ. Health 92, 37–48. 10.1007/s00420-018-1360-1. [PubMed: 30293089]

Wang B, Chai G, Sha Y, Su Y, 2022. Association between ambient temperature and cardiovascular disease hospitalisations among farmers in suburban northwest China. Int. J. Biometeorol 66, 1317–1327. 10.1007/s00484-022-02278-2. [PubMed: 35381858]

Wang B, Chai G, Sha Y, Zha Q, Su Y, Gao Y, 2021. Impact of ambient temperature on cardiovascular disease hospital admissions in farmers in China's Western suburbs. Sci. Total Environ 761, 143254 10.1016/J.SCITOTENV.2020.143254. [PubMed: 33190905]

Weilnhammer V, Schmid J, Mittermeier I, Schreiber F, Jiang L, Pastuhovic V, Herr C, Heinze S, 2021. Extreme weather events in europe and their health consequences – A systematic review. Int. J. Hyg. Environ. Health 233, 113688. 10.1016/J.IJHEH.2021.113688. [PubMed: 33530011]

Xu Z, Cheng J, Hu W, Tong S, 2018. Heatwave and health events: A systematic evaluation of different temperature indicators, heatwave intensities and durations. Sci. Total Environ 630, 679–689. 10.1016/j.scitotenv.2018.02.268. [PubMed: 29494976]

Yang J, Yin P, Zhou M, Ou CQ, Guo Y, Gasparrini A, Liu Y, Yue Y, Gu S, Sang S, Luan G, Sun Q, Liu Q, 2015. Cardiovascular mortality risk attributable to ambient temperature in China. Heart 101, 1966–1972. 10.1136/heartjnl-2015-308062. [PubMed: 26567233]

Zhang H, Liu L, Zeng Y, Liu M, Bi J, Ji JS, 2021. Effect of heatwaves and greenness on mortality among Chinese older adults. Environ. Pollut 290, 118009 10.1016/j.envpol.2021.118009. [PubMed: 34523521]

Zhao L, Oppenheimer M, Zhu Q, Baldwin JW, Ebi KL, Bou-Zeid E, Guan K, Liu X, 2018a. Interactions between urban heat islands and heat waves. Environ. Res. Lett 13, 034003 10.1088/1748-9326/aa9f73.

Zhao Q, Zhao Y, Li S, Zhang YY, Wang Q, Zhang H, Qiao H, Li W, Huxley R, Williams G, Zhang YY, Guo Y, 2018b. Impact of ambient temperature on clinical visits for cardio-respiratory diseases in rural villages in northwest China. Sci. Total Environ 612, 379–385. 10.1016/J.SCITOTENV.2017.08.244. [PubMed: 28858748]

Zhu D, Zhou Q, Liu M, Bi J, 2021. Non-optimum temperature-related mortality burden in China: Addressing the dual influences of climate change and urban heat islands. Sci. Total Environ 782, 146760 10.1016/J.SCITOTENV.2021.146760. [PubMed: 33836376]
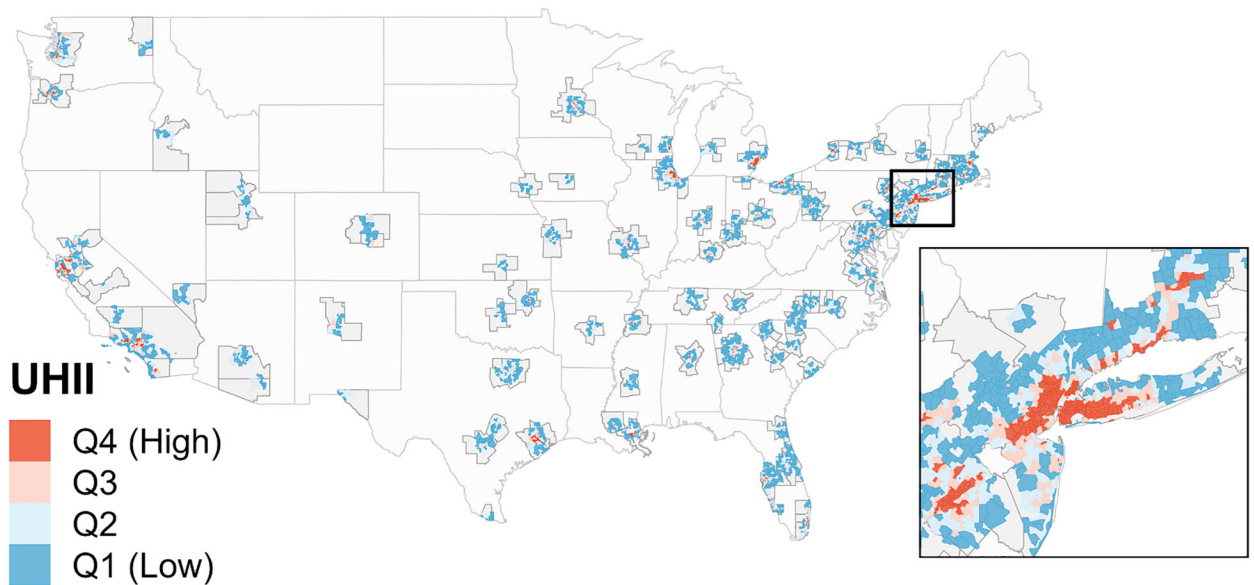
Fig. 1.

The 120 metropolitan statistical areas (MSAs) in the contiguous US, with 9,917 ZIP codes located in their urban cores. ZIP codes are shown with their associated surface urban heat island intensity (UHII) level, defined using UHII quartiles (Q1 = Quartile 1), weighted to each have 25% of all cardiovascular disease hospitalizations. Dark grey outlines indicate the MSA boundaries; red and blue areas indicate the ZIP codes that overlapped an urban core of an MSA and were included in the analysis; light grey areas within the MSA boundaries indicate areas that did not overlap an urban core and were excluded from analysis. The inset is centered on the New York-Jersey City-White Plains, NY-NJ MSA and displays ZIP codes across 10 different MSAs.
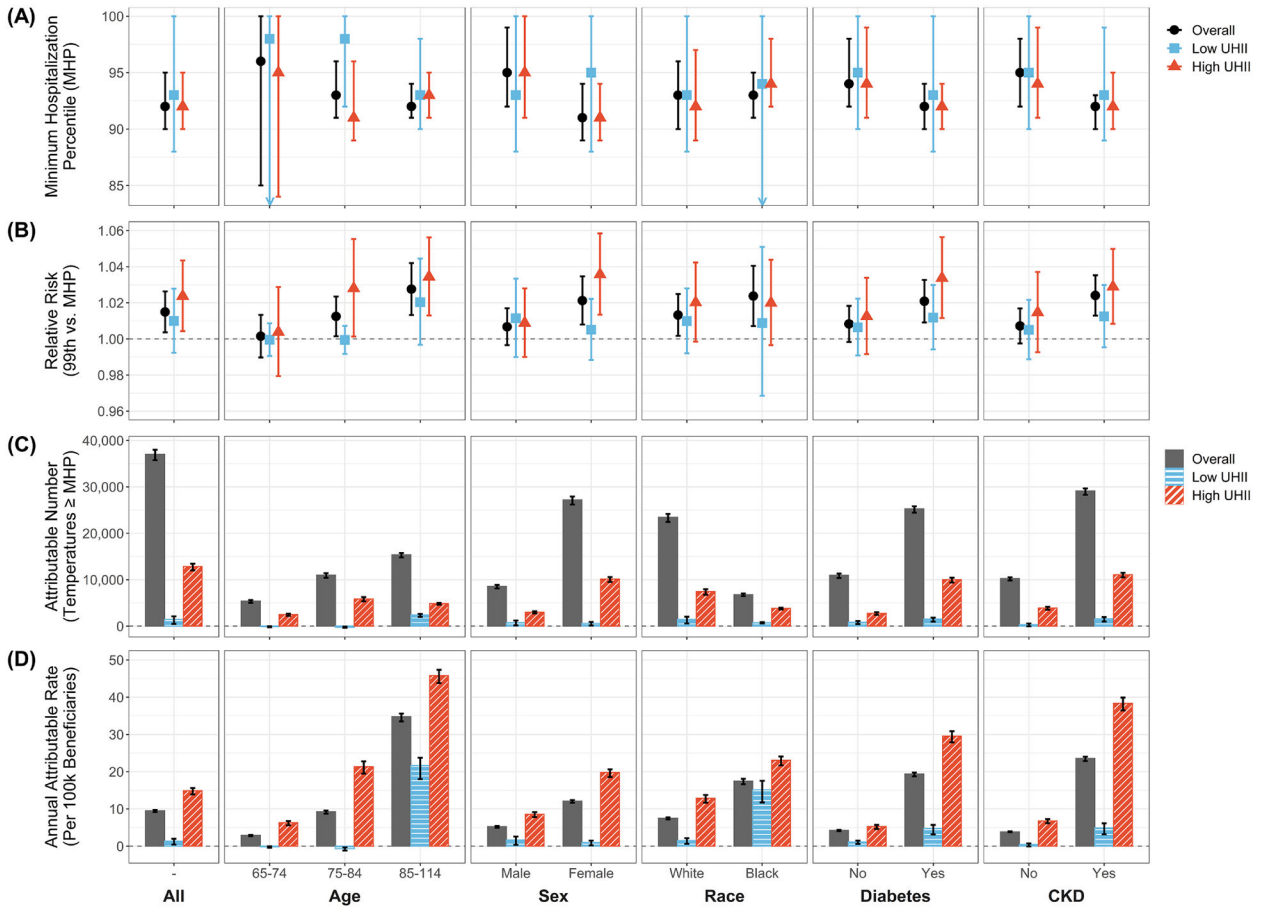
Fig. 2.
The (A) minimum hospitalization percentile (MHP), (B) 21-day cumulative relative risk
at extreme heat (99th ambient temperature percentile compared to the MHP), and (C)
number and (D) annual rate per 100,000 Medicare beneficiaries of heat-attributable (ambient
temperatures above the MHP) cardiovascular disease hospitalizations across the urban cores
of 120 metropolitan statistical areas in the contiguous US, 2000–2017. Results are shown for
the entire study population and by age, sex, race, and diabetes and chronic kidney disease
(CKD) status, overall and in low and high urban heat island intensity (UHII) areas. The
associated numeric results can be found in Table S2.
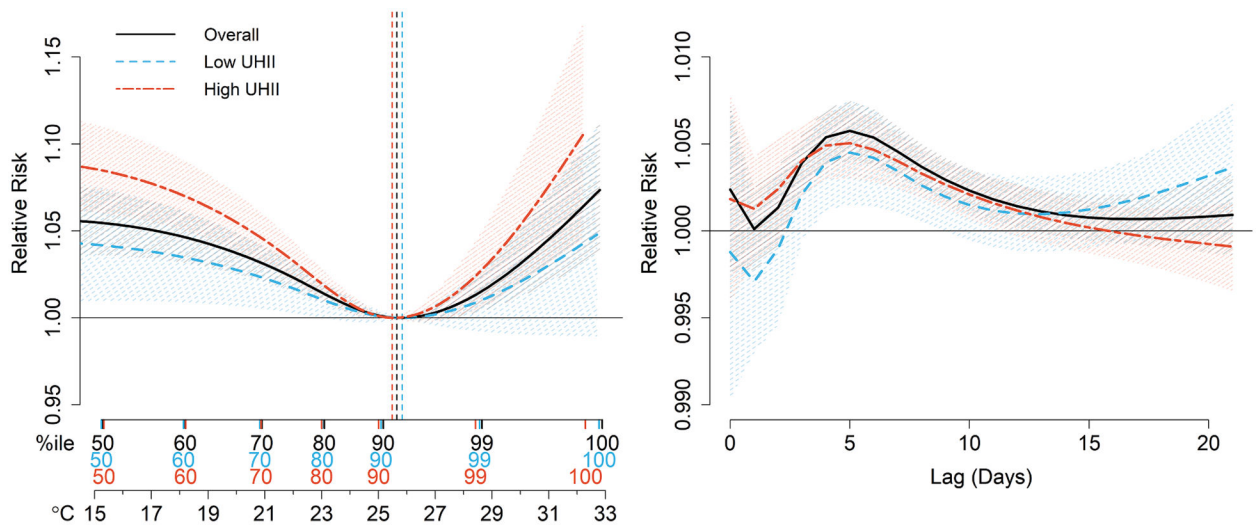
Fig. 3.

The 21-day cumulative exposure–response [left] and extreme heat (99th ambient temperature percentile) lag-response [right] associations between daily mean ambient temperature and daily hospitalizations for cardiovascular disease, overall and in low and high urban heat island intensity (UHII) areas. Results are shown for the entire study population across the urban cores of 120 metropolitan statistical areas in the contiguous US, 2000–2017. The vertical dashed lines indicate the location of the minimum hospitalization percentile.
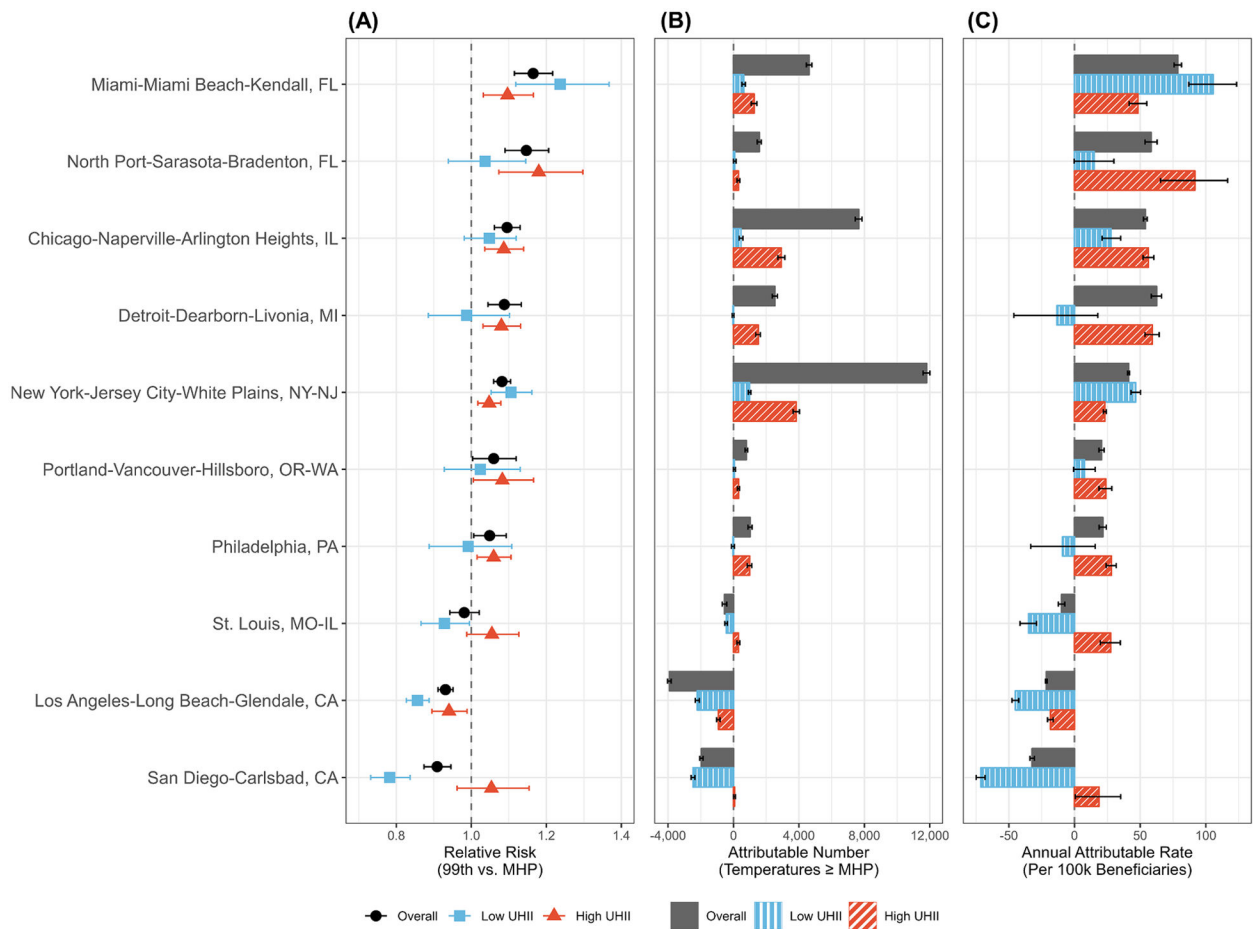
Fig. 4.

The (A) 21-day cumulative relative risk (RR) at extreme heat (99th ambient temperature percentile compared to the MHP) and (B) number and (C) annual rate per 100,000 Medicare beneficiaries of heat-attributable (ambient temperatures above the MHP) cardiovascular disease (CVD) hospitalizations in the urban cores of 10 metropolitan statistical areas (MSAs), 2000–2017. Results are shown overall and in low and high urban heat island intensity (UHII) areas. The 10 MSAs displayed were selected to demonstrate the variability in the overall and UHII-specific heat-related CVD risk and burden and are arranged in descending order by overall extreme heat RR. The results for all 120 MSAs can be found in Fig. S7 and Table S3.

Table 1

Characteristics of the study population and exposure data, overall and in low and high urban heat island intensity (UHII) areas, in the urban cores of 120 metropolitan statistical areas (MSAs) in the contiguous US, 2000–2017.

Characteristic	Overall	Low UHII	High UHII
Surface UHII (°C)			
Range	−9.3–10.3	−9.3–0.5	3.9–10.3
Mean (IQR)	1.8 (3.7)	−1.0 (1.5)	5.6 (1.8)
MSAs, #	120	120	98
ZIP Codes, #	9,917	3,271	2,144
Beneficiaries, # [a]	21,618,077	5,918,402	4,796,597
CVD Hospitalizations, # (%) [b]			
Total	48,631,055 (100)	12,166,601 (100)	12,144,510 (100)
Age			
65–74	14,966,997 (30.8)	3,890,932 (32.0)	3,713,530 (30.6)
75–84	19,606,673 (40.3)	4,900,894 (40.3)	4,875,416 (40.1)
85–114	13,969,100 (28.7)	3,355,087 (27.6)	3,544,507 (29.2)
Sex			
Female	27,758,003 (57.1)	6,667,264 (54.8)	7,224,044 (59.5)
Male	20,836,918 (42.8)	5,493,715 (45.2)	4,916,936 (40.5)
Race			
White	39,392,718 (81.0)	10,897,789 (89.6)	8,207,103 (67.6)
Black	5,945,058 (12.2)	672,026 (5.5)	2,746,097 (22.6)
Diabetes			
Yes	25,980,128 (53.4)	5,990,226 (49.2)	7,308,779 (60.2)
No	22,605,580 (46.5)	6,164,866 (50.7)	4,833,500 (39.8)
Chronic Kidney Disease			
Yes	28,469,413 (58.5)	6,858,978 (56.4)	7,382,643 (60.8)
No	20,115,414 (41.4)	5,297,028 (43.5)	4,757,851 (39.2)
Ambient Temperature (°C) [c]			
Mean (IQR)	14.8 (14.1)	14.4 (14.1)	14.4 (14.1)
99th Percentile	28.6	28.4	28.3

EPA Author Manuscript

EPA Author Manuscript

EPA Author Manuscript

Note: There were no missing values in the UHII, Medicare, or ambient temperature datasets.

[a] Average of the annual number of Medicare beneficiaries, 2000–2017.

[b] Total number of CVD hospitalizations between 2000 and 2017.

[c] Values calculated by using ZIP code-level data to first obtain MSA-specific values and then averaging all MSA-specific values.